Shifting media for carpet cloaks, antiobject independent illusion optics, and a restoring device

XiaoFei Zang, Bin Cai, and YiMing Zhu*

Engineering Research Center of Optical Instrument and System, Ministry of Education and Shanghai Key Laboratory of Modern Optical System, University of Shanghai for Science and Technology, No. 516 JunGong Road, Shanghai 200093, China

*Corresponding author: ymzhu@usst.edu.cn

Received 17 December 2012; revised 21 January 2013; accepted 23 January 2013; posted 24 January 2013 (Doc. ID 181889); published 13 March 2013

In traditional cases, the basic principle of carpet cloak is that a two-dimensional bump above ground plane is compressed into a one-dimensional line which is close to the ground plane. As a result, the bump can be hidden. In this paper, different from the traditional carpet cloak, we propose a shifting media to achieve the carpet cloak. By covering with the shifting media, an object floating on a ground plane can be directly shifted beneath the ground plane (rather than compressing it into a line), resulting in a floating carpet cloak. Antiobject independent illusion optics, i.e., turning an object into another one without any antiobjects, can be realized based on this kind of shifting media. As an application of the shifting media, a restoring device, by which the broken objects (such as antiques) can be perfectly restored, is also investigated. © 2013 Optical Society of America

OCIS codes: 160.3918, 230.0230, 260.2710.

1. Introduction

In the past few years, transformation optics [1–14] has attracted much attention, due to its potential applications for manipulating the transmission path of electromagnetic waves. Based on the transformation optics, invisible cloaks, one of the most important and typical applications, were proposed in theory [1–5]. Subsequently, microwave, terahertz, and optical cloaks were experimentally realized [6–14]. In addition, great progress has been made on different kinds of cloaks in recent years, such as square cloaks, elliptic cloaks, arbitrary-shaped cloaks, multilayer cylinder cloaks, and the general open-closed cloaks [15–19]. Recently, another interesting phenomenon of super-scattering, which means that an object seemed bigger than its real geometric size by covering with complementary media, has been reported in [20]. In contrast to the above internal cloaks, an antiobject dependent external cloak, which could make an object outside its domain be invisible, was investigated by virtue of the complementary media [21]. Many other kinds of applications, such as superabsorbers, tunable electromagnetic gateways, overlapped optics, and so on, were also studied [22–27]. Furthermore, the complementary media theory has also been developed to hide objects floating upon a ground plane [28]. Such a device aims to camouflage an object by generating a remote virtual perfect electric conductor (PEC) sheet, which is similar to the carpet cloak. The basic principle of this phenomenon is that the complementary media can guide electromagnetic waves around a closed region and keep an electric field normal to its conducting surface. Therefore, the shape of the hidden object must be consistent with the folding shape between the complementary media region and the compression region. In other words, when the distance between the upper surface of hidden object and the PEC ground

1559-128X/13/091832-06$15.00/0

plane is fixed, the complementary media is only effective for the cloaking of some shape-fixed objects and is not good for hiding objects with arbitrary shapes. Furthermore, the basic principle of this and the traditional carpet cloaks is that the hidden objects are compressed into a one-dimensional line which is close to the ground plane. In addition, this kind of complementary media is also applied to design illusion optics, i.e., an object appears to be some other object [27]. But it is dependent on the antiobject. So, Jiang *et al.* proposed another way to design antiobject independent illusion optics [29,30]. However, the antiobject independent illusion optics in [29,30] were based on the anisotropic and inhomogeneous transformation media. In view of these problems, we propose an anisotropic but homogeneous shifting media to design carpet cloak and antiobject independent illusion optics. Although another kind of shifting media is proposed in [31], the object can just be shifted inside the transformation media region. Thus, it can hardly be applied to designing a carpet cloak. Rather than compressing the hidden object into a line, the object covered with the shifting media is directly shifted below the ground plane. Although the distance between the up surface of the hidden object and the ground plane is fixed, our shifting media is beneficial for cloaking objects with arbitrary shapes. Another kind of application of the shifting media, i.e., a restoring device, is also studied for the purpose of the restoration of broken objects (such as antiques).

2. Theoretical Model

The schematic of the shifting media is shown in Fig. 1, where a small trapezoidal object (region V in Fig. 1 with $\varepsilon = \mu = 1$) is covered with a trapezoidal shifting media shell (gray shell). The regions of $A_1'B_1'B_2A_2$, $A_1'A_2D_2D_1'$, $B_1'B_2C_2C_1'$, $C_1'C_2D_2D_1'$, are mapped into regions of $A_1B_1B_2A_2$, $A_1A_2D_2D_1$, $B_1B_2C_2C_1$, $C_1C_2D_2D_1$, respectively, due to the shifting media. Here, the coordinates in Fig. 1 are: $A_1(-c_{11}, -h_{11}), B_1(c_{11}, -h_{11}), C_1(c_{12}, h_{11}), D_1(-c_{12}, h_{11})$, $A_2(-c_{21}, -h_{21})$, $B_2(c_{21}, -h_{21})$, $C_2(c_{22}, h_{21})$, and $D_2(-c_{22}, h_{21})$. According to the theory of transformation optics, the coordinate transformation between the virtual space and the physical space can be expressed as:

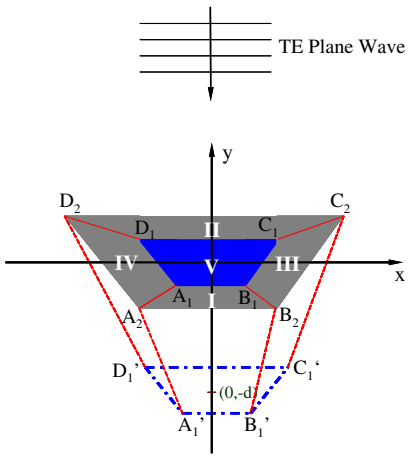

Fig. 1. (Color online) Schematic of the shifting media in two-dimensional view. The inner (core) blue region is an object while the gray region is the shifting media. The blue core region $A_1B_1C_1D_1$ can be moved to region $A_1'B_1'C_1'D_1'$. Both of these two regions are separated with a distance d.

In region I:

$$x' = x \qquad y' = \frac{(h_{21} - h_{11})y + d * h_{21}}{h_{21} - h_{11} - d}, \qquad z' = z, \quad (1)$$

In region II:

$$x' = x \qquad y' = \frac{(h_{21} - h_{11})y + d * h_{21}}{h_{21} - h_{11} + d}, \qquad z' = z, \quad (2)$$

In region III:

$$x' = x$$
$$y' = y + \frac{d * [c_{21} + (c_{22} - c_{21})(y' + h_{21})/2h_{21} - x]}{c_{21} - c_{11} + (c_{22} - c_{21})(h_{21} - h_{11})/2h_{21}}, \quad (3)$$
$$z' = z,$$

In region IV:

$$x' = x$$
$$y' = y + \frac{d * [c_{21} + (c_{22} - c_{21})(y' + h_{21})/2h_{21} + x]}{c_{21} - c_{11} + (c_{22} - c_{21})(h_{21} - h_{11})/2h_{21}}, \quad (4)$$
$$z' = z.$$

The corresponding permittivity and permeability tensors of the transformation media are given as follows:

In region I:

$$\frac{\bar{\bar{\varepsilon}}}{\varepsilon} = \frac{\bar{\bar{\mu}}}{\mu} = \begin{bmatrix} 1/m_1 & 0 & 0 \\ 0 & m_1 & 0 \\ 0 & 0 & 1/m_1 \end{bmatrix}, \quad (5)$$

In region II:

$$\frac{\bar{\bar{\varepsilon}}}{\varepsilon} = \frac{\bar{\bar{\mu}}}{\mu} = \begin{bmatrix} 1/m_2 & 0 & 0 \\ 0 & m_2 & 0 \\ 0 & 0 & 1/m_2 \end{bmatrix}, \quad (6)$$

In region III:

$$\frac{\bar{\bar{\varepsilon}}}{\varepsilon} = \frac{\bar{\bar{\mu}}}{\mu} = \begin{bmatrix} 1 - m_3 & -m_4 & 0 \\ -m_4 & (1 + m_4^2)/(1 - m_3) & 0 \\ 0 & 0 & 1 - m_3 \end{bmatrix}, \quad (7)$$

In region IV:

$$\frac{\bar{\bar{\varepsilon}}}{\varepsilon} = \frac{\bar{\bar{\mu}}}{\mu} = \begin{bmatrix} 1 - m_3 & m_4 & 0 \\ m_4 & (1 + m_4^2)/(1 - m_3) & 0 \\ 0 & 0 & 1 - m_3 \end{bmatrix}, \quad (8)$$

where $m_1 = \frac{h_{21}-h_{11}}{h_{21}-h_{11}-d}$, $m_2 = \frac{h_{21}-h_{11}}{h_{21}-h_{11}+d}$, $m_3 = \frac{d*(c_{22}-c_{21})}{2h_{21}*(c_{21}-c_{11}+(c_{22}-c_{21})(h_{21}-h_{11})/2h_{21})}$, and $m_4 = \frac{d}{2h_{21}*(c_{21}-c_{11}+(c_{22}-c_{21})(h_{21}-h_{11})/2h_{21})}$. Here, we want to emphasize that these parameters in Eqs. (5)–(8) are also appropriate for the case when the center of the shifting media is not located at (0, 0). The detailed system parameters in Fig. 1 are $c_{11} = 0.5$ m, $h_{11} = 0.25$ m, $c_{12} = 1$ m, $h_{21} = 0.5$ m, $c_{21} = 1$ m, $c_{22} = 2$ m. Taking $d = 1$ m for example, the numerical values of the variables of m_1, m_2, m_3, m_4 are as follows: $m_1 = -1/3, m_2 = 1/5, m_3 = m_4 = 4/3$. From Eqs. (5)–(8), we can find that the shifting media is anisotropic but homogeneous. Based on the rotation transformation [29], the dielectric tensor in region III and IV can be diagonalized. The material parameters with eigenbasis can be written as

$$\begin{aligned}\varepsilon_x &= \frac{\varepsilon'_{xx} + \varepsilon'_{yy} - \sqrt{(\varepsilon'_{xx} - \varepsilon'_{yy})^2 + 4\varepsilon'^2_{xy}}}{2}\\ \varepsilon_y &= \frac{\varepsilon'_{xx} + \varepsilon'_{yy} + \sqrt{(\varepsilon'_{xx} - \varepsilon'_{yy})^2 + 4\varepsilon'^2_{xy}}}{2}\\ \varepsilon_z &= \varepsilon'_{zz}, \end{aligned} \tag{9}$$

where $\varepsilon'_{xx} = 1 - m_3$, $\varepsilon'_{yy} = (1 + m_4^2)/(1 - m_3)$, $\varepsilon'_{xx} = \mp m_4$ ("−" represents region III and "+" represents region IV), and $\varepsilon'_{zz} = 1 - m_3$. The magnetic permeability of μ_x, μ_y and μ_z have the similar expression. For $d = 1$ m, the axis of the material is 80.8° counterclockwise rotation in region III (99.2° for region IV).

3. Numerical Simulation and Discussion

First, we carry out finite element simulations to demonstrate the shifting effect of shifting media. Figure 2(a) shows the field distribution of shifting media when a transverse electric (TE) plane wave irradiates on the shifting media with an incident angle of 45° for the wavelength of 0.4 m. In this case, the central region (region V in Fig. 1) is air whose permittivity and permeability are $\varepsilon = \mu = 1$. It can be found that the field distribution in the central region is the same as the region encircled by the black dash-dotted border. This means that the electric field below the shifting media is folded into the central region V. Figure 2(b) depicts the scattered field distribution of a bare PEC with its center located at (0, 0.15 m). Obviously, strongly scattered wave appears in the electric field distribution, as shown in Fig. 2(b). In Fig. 2(c), we display the scattered field distribution of the same PEC for its center located at (0, 1.15 m) which is coated by a shifting media shell. The comparison of the far-field Figs. 2(b) and 2(c) is shown in Fig. 2(d); both far-field distributions and far-field scattered patterns of these two PECs (although both of them are at different places) are nearly the same. Here, slight noncoincidence of far-field scattered patterns can be explained as follows: the polygonal meshes we set in the Comsol software in our computing platform is too coarse. This indicates that the PEC in Fig. 2(c) is effectively moved 1 m down by covering the shifting media shell.

Based on the shifting media, one of the most important applications, a floating carpet cloak, can be realized. Figure 3(a) shows the field distribution when a 0.75 GHz Gaussian beam irradiates on a PEC ground

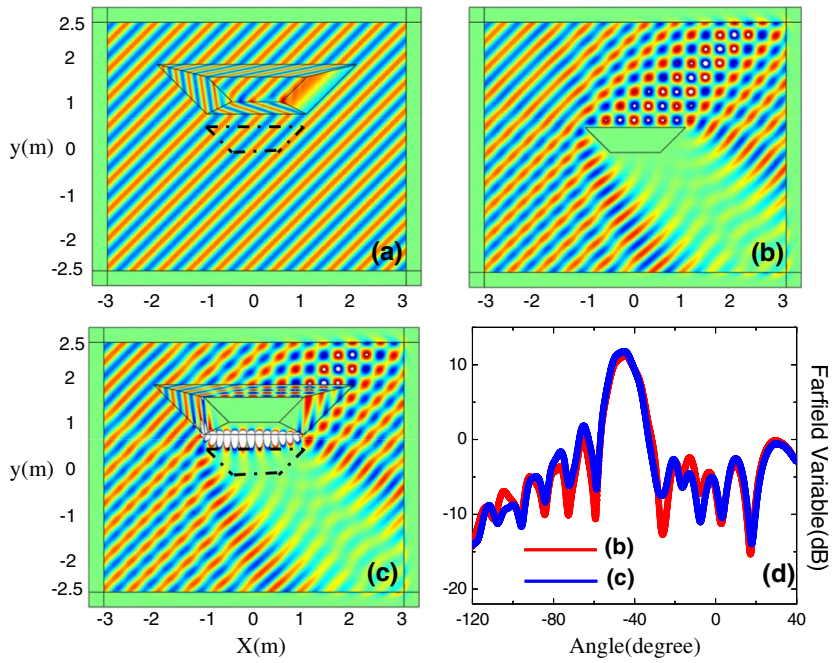

Fig. 2. (Color online) Electric field distribution of the shifting media ($d = 1$ m), when the center region (region V) is embedded with (a) free space or (c) PEC, and the incident plane wave moves from left to right with tilt angle of 45°. (b) Electric field distribution of the PEC without the shifting media shell. (d) The corresponding scattered patterns of (a)–(c).

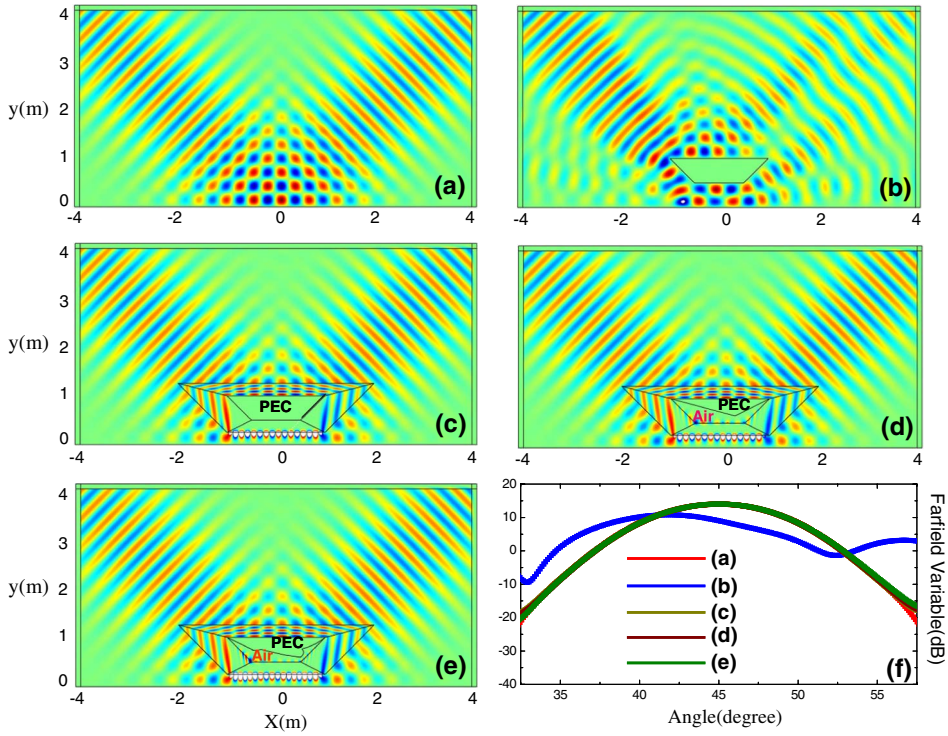

Fig. 3. (Color online) (a) Electric field distribution when a Gaussian beam is launched at 45° toward the ground in the case of $d = 1$ m. (b) Electric field distribution when a bare trapezoidal-shaped PEC is present above the ground plane. (c) The same as (b) but the PEC is covered with a shifting media shell. (d) and (e) The same as (c) but with triangular-shaped and arbitrary-shaped PEC, respectively. (f) The corresponding far-field scattered patterns of (a)–(e).

plane with the incident angle 45°. When a bare trapezoidal PEC is placed above this ground plane, a strongly scattered wave can be clearly observed in the electric distribution [Fig. 3(b)]. Figure 3(c) depicts the field distribution of the same PEC covered with the shifting media shell. Comparing Figs. 3(a) and 3(c), we can find that both of them have the same far-field distribution [also see the same far-field scattered patterns in Fig. 3(f)] except for in the transformation region. Therefore, the PEC floating upon the ground plane is hidden. In other words, the shifting media shell acts as a floating carpet cloak, which moves the upper surface of the PEC down to the ground plane. In Figs. 3(d) and 3(e), we also carry out the finite element simulations to demonstrate the function of the floating carpet cloak with triangular-shaped and arbitrary-shaped PECs, respectively. Comparing Figs. 3(a), 3(c)–3(e) and the corresponding far-field scattered patterns in Fig. 3(f), all of them nearly have the same far-field distribution. These demonstrate that PECs, whether trapezoidal or triangular or arbitrary shaped, can be hidden by covering with the shifting media shell.

Now, we discuss the antiobject independent illusion optics, i.e., turning a spoon-shaped object into an arrow-shaped object without utilizing any antiobject media. Figures 4(a) and 4(c) show the field distribution of a dielectric spoon ($\varepsilon = 2.5$, $\mu = 1$) and an arrow-shaped PEC located in free space ($\varepsilon = \mu = 1$), respectively. Strongly scattered fields appear behind these two objects. Figure 4(b) depicts the corresponding field distribution of the same spoon covered with the shifting media, and at the same time, an arrow-shaped object is embedded in region II (the compression region). Comparing Figs. 4(b) and 4(c), both of them have the same far-field pattern shown in Fig. 4(e) (red and blue curves). It means that the dielectric spoon in Fig. 4(b) is changed into an arrow-shaped object, because the spoon in Fig. 4(b) is directly shifted below the lower surface of free space [see Fig. 4(d): the spoon is invisible]. Therefore, this kind of illusion optics does not rely on the antiobject to cancel the corresponding scattered field of the hidden object.

Finally, we investigate another application of the shifting media: a restoring device (or seamless connector). Such a kind of restoring device can be applied to restore broken objects. In Fig. 5(a), we display the scattered field of a PEC bottle. A significantly scattered wave appears in the scattered field distribution; the corresponding far-field scattered pattern is shown in Fig. 5(d) by the red curve. Figure 5(b) shows the scattered field distribution of the broken bottle, where the bottle is divided into two parts. Comparing Figs. 5(a) and 5(b), both of them have different far-field distributions. But, when one part of the broken bottle is covered with the shifting media, the far-field distribution of the broken one recovers to the same as that of the original one, as shown in Fig. 5(c) [see the far-field patterns in

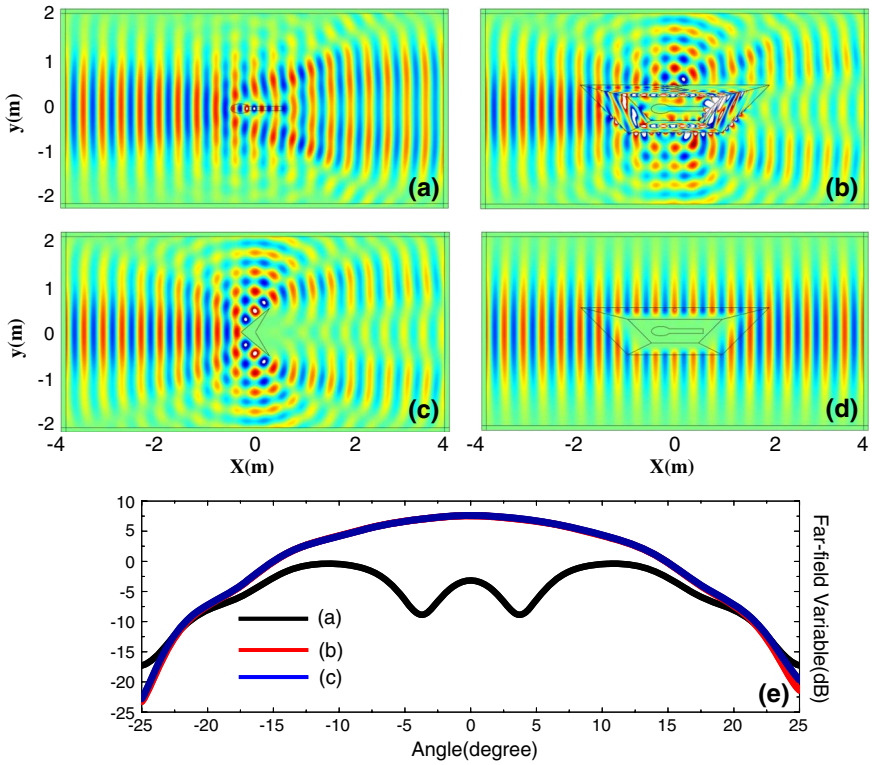

Fig. 4. (Color online) (a) Electric field distribution when a Gaussian beam is launched from the left side with just a bare dielectric spoon in free space for $d = 2.25$ m. (b) The same as (a) but the spoon is covered with a shifting media shell and an arrow-shaped object is embedded in the compression region. (c) Electric field distribution when a Gaussian beam is launched from the left side with just a bare arrow-shaped object (PEC) in free space. (d) The same as (b) but without the arrow-shaped object. (e) The corresponding far-field scattered patterns of (a)–(c).

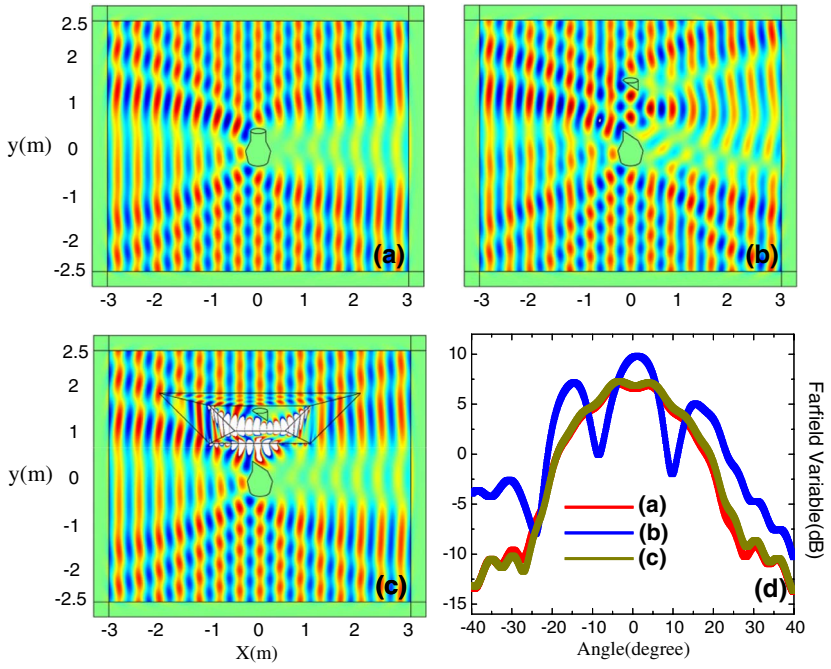

Fig. 5. (Color online) (a) Electric field distribution when a plane wave is launched toward a porcelain bottle from the left for $d = 1.5$ m. (b) Electric field distribution when the porcelain bottle is divided into two parts. (c) The same as (b), but one part of the broken porcelain bottle is covered with shifting media. (d) The corresponding far-field scattered patterns of (a)–(c).

Fig. 5(d) marked as red and dark yellow curves]. This indicates that the broken bottle is restored as a perfect unbroken bottle. This property may open a new perspective for restoring valuable antiques.

4. Conclusion

In summary, we have theoretically proposed a kind of shifting media which can hide the floating object with arbitrary shapes by shifting the object beneath ground plane. Such a kind of shifting media can be applied to design antiobject independent illusion optics, i.e., turning a spoon-shaped object into an arrow-shaped object. Another potential application of this shifting media, such as restoration of broken objects, has also been discussed in detail. Both the theory model and numerical simulations demonstrate that this shifting media has many promising applications in the field of transformation optics devices.

This work is partly supported by the Major National Development Project of Scientific Instrument and Equipment (2011YQ150021), the Key Scientific and Technological Project of Science and Technology Commission of Shanghai Municipality (11DZ1110800), National Natural Science Foundation of China (11174207, 61138001, 61007059, 61205094), the Leading Academic Discipline Project of Shanghai Municipal Government (S30502) and the Key Project of the Shanghai Municipal Science and Technology Commission (12JC1407100).

References

1. J. B. Pendry, D. Schurig, and D. R. Smith, "Controlling electromagnetic fields," Science **312**, 1780–1782 (2006).
2. U. Leonhardt, "Optical conformal mapping," Science **312**, 1777–1780 (2006).
3. W. Cai, U. K. Chettiar, A. V. Kildishev, and V. M. Shalaev, "Optical cloaking with metamaterials," Nat. Photonics **1**, 224–227 (2007).
4. J. Li and J. B. Pendry, "Hiding under the carpet: a new strategy for cloaking," Phys. Rev. Lett. **101**, 203901 (2008).
5. H. Y. Chen, C. T. Chan, and P. Shen, "Transformation optics and metamaterials," Nat. Mater. **9**, 387–396 (2010).
6. D. Schurig, J. J. Mock, B. J. Justice, S. A. Cummer, J. B. Pendry, A. F. Starr, and D. R. Smith, "Metamaterial electromagnetic cloak at microwave frequencies," Science **314**, 977–980 (2006).
7. R. Liu, C. Ji, J. J. Mock, J. Y. Chin, T. J. Cui, and D. R. Smith, "Broadband ground-plane cloak," Science **323**, 366–369 (2009).
8. J. Valentine, J. Li, T. Zentgraf, G. Bartal, and X. Zhang, "An optical cloak made of dielectrics," Nat. Mater. **8**, 568–571 (2009).
9. L. H. Gabrielli, J. Cardenas, C. B. Poitras, and M. Lipson, "Silicon nanostructure cloak operating at optical frequencies," Nat. Photonics **3**, 461–463 (2009).
10. H. F. Ma and T. J. Cui, "Three-dimensional broadband ground plane cloak made of matematerials," Nat. Commun. **1**, 21–26 (2010).
11. X. Z. Chen, Y. Luo, J. J. Zhang, K. Jiang, J. B. Pendry, and S. Zhang, "Macroscopic invisibility cloaking of visible light," Nat. Commun. **2**, 176–181 (2011).
12. B. L. Zhang, Y. Luo, X. G. Liu, and G. Barbastathis, "Macroscopic invisibility cloak for visible light," Phys. Rev. Lett. **106**, 033901 (2011).
13. F. Zhou, Y. Bao, W. Cao, C. T. Stuart, J. Gu, W. L. Zhang, and C. Sun, "Hiding a realistic object using a broadband terahertz invisibility cloak," Sci. Rep. **1**, 78–82 (2011).
14. D. Liang, J. Gu, J. Han, Y. Yang, S. Zhang, and W. L. Zhang, "Robust large dimension terahertz cloaking," Adv. Mater. **24**, 916–921 (2012).
15. M. Rahm, D. Schurig, D. A. Roberts, S. A. Cummer, D. R. Smith, and J. B. Pendry, "Design of electromagnetic cloaks and concentrators using form-invariant coordinate transformations of Maxwell's equations," Photon. Nanostruct. Fundam. Applic. **6**, 87–95 (2008).
16. W. X. Jiang, T. J. Cui, G. X. Yu, X. Q. Lin, Q. Cheng, and J. Y. Chin, "Arbitrarily elliptical-cylindrical invisible cloaking," J. Phys. D **41**, 085504 (2008).
17. C. Li, K. Yao, and F. Li, "Two-dimensional electromagnetic cloaks with non-conformal inner and outer boundaries," Opt. Express **16**, 19366–19374 (2008).
18. B. Ivsic, Z. Sipus, and S. Hrabar, "Analysis of uniaxial multilayer cylinders used for invisible cloak realization," IEEE Trans. Antennas Propag. **57**, 1521–1527 (2009).
19. T. Han, C. W. Oiu, and X. H. Tang, "The general two-dimensional open-closed cloak with tunable inherent discontinuity and directional communication," Appl. Phys. Lett. **97**, 124104 (2010).
20. T. Yang, H. Y. Chen, X. Luo, and H. Ma, "Superscatterer: enhancement of scattering with complementary media," Opt. Express **16**, 18545–18550 (2008).
21. Y. Lai, H. Y. Chen, Z. Q. Zhang, and C. T. Chan, "Complementary media invisibility cloak that cloaks objects at a distance outside the cloaking shell," Phys. Rev. Lett. **102**, 093901 (2009).
22. J. Ng, H. Y. Chen, and C. T. Chan, "Metamaterial frequency-selective superabsorber," Opt. Lett. **34**, 644–646 (2009).
23. H. Y. Chen, X. Zhang, X. Luo, H. Ma, and C. T. Chan, "A simple route to a tunable electromagnetic gateway," New. J. Phys. **10**, 083012 (2009).
24. K. Wu and G. P. Wang, "General insight into the complementary media-based camouflage devices from Fourier optics," Opt. Lett. **35**, 2242–2244 (2010).
25. J. S. Mei, Q. Wu, and K. Zhang, "Multifunction complementary cloak with homogeneous anisotropic material parameters," J. Opt. Soc. Am. B. **29**, 2067–2073 (2012).
26. Y. D. Xu, S. W. Du, L. Gao, and H. Y. Chen, "Overlapped illusion optics: a perfect lens brings a brighter feature," New. J. Phys. **13**, 023010 (2011).
27. Y. Lai, J. Ng, H. Y. Chen, D. Han, J. Xiao, Z. Zhang, and C. T. Chan, "Illusion optics: the optical transformation of an object into another object," Phys. Rev. Lett. **102**, 253902 (2009).
28. J. J Zhang, Y. Luo, and N. A. Mortensen, "Hiding levitating objects above a ground plane," Appl. Phys. Lett. **97**, 133501 (2010).
29. W. X. Jiang, H. F. Ma, Q. Cheng, and T. J. Cui, "Illusion media: generating virtual objects using realizable metamaterials," Appl. Phys. Lett. **96**, 121910 (2010).
30. W. X. Jiang and T. J. Cui, "Radar illusion via metamaterials," Phys. Rev. E. **83**, 026601 (2011).
31. W. X. Jiang and T. J. Cui, "Moving targets virtually via composite optical transformation," Opt. Express **18**, 5161–5167 (2010).